



Article

Experimental and Theoretical Insight into Different Species of p-Aminothiophenol Adsorbed on Silver Nanoparticles

María Rosa López-Ramírez ^{1,*}, Laura García-Gómez ², Arantxa Forte-Castro ³ and Rafael Contreras-Cáceres ³ ¹ Department of Physical Chemistry, Faculty of Science, University of Málaga, 29071 Málaga, Spain² UMALASERLAB, Department of Analytical Chemistry, University of Málaga, C/ Jiménez Fraud 4, 29010 Málaga, Spain; laugargom@uma.es³ Department of Chemistry and Physics, Faculty of Experimental Sciences, University of Almeria, 04120 Almería, Spain; afc325@ual.es (A.F.-C.); rcc689@ual.es (R.C.-C.)

* Correspondence: mrlopez@uma.es

Abstract: The adsorption of p-aminothiophenol (PATP) on metallic nanostructures is a very interesting phenomenon that depends on many factors, and because of that, PATP is an increasingly important probe molecule in surface-enhanced Raman spectroscopy (SERS) due to its strong interaction with Ag and Au, its intense SERS signal, and its significance in molecular electronics. In our study, the SERS spectra of PATP on silver colloids were investigated and we considered several factors, such as the effect of the adsorbate concentration, the nature of the metallic nanoparticles, and the excitation wavelength. Differences between the SERS spectra recorded at high and low concentrations of PATP were explained and DFT calculations of different species were performed in order to support the experimental results. Additionally, time-dependent density-functional theory (TD-DFT) calculations were used to simulate the UV spectra of each species and to determine the MOs involved in each transition. The presence of different species of PATP adsorbed onto the metal surface gave rise to the acquisition of simultaneous SERS signals from those species and the consequent overlapping of some bands with new SERS bands coming from the dimerization of PATP. This work helped to discern which species is responsible for each SERS spectrum under particular experimental conditions.

Keywords: SERS; silver nanoparticles; p-aminothiophenol; DFT; TD-DFT



Citation: López-Ramírez, M.R.; García-Gómez, L.; Forte-Castro, A.; Contreras-Cáceres, R. Experimental and Theoretical Insight into Different Species of p-Aminothiophenol Adsorbed on Silver Nanoparticles. *Spectrosc. J.* **2024**, *2*, 145–153. <https://doi.org/10.3390/spectroscj2030009>

Academic Editors: Rui Fausto and Turrell Sylvia

Received: 6 June 2024

Revised: 18 July 2024

Accepted: 25 July 2024

Published: 28 July 2024



Copyright: © 2024 by the authors. Licensee MDPI, Basel, Switzerland. This article is an open access article distributed under the terms and conditions of the Creative Commons Attribution (CC BY) license (<https://creativecommons.org/licenses/by/4.0/>).

1. Introduction

Since surface-enhanced Raman spectroscopy (SERS) was casually discovered by Fleischmann et al. in 1974 [1–3], many improvements to the Raman technique have occurred. Currently, SERS spectroscopy is one of the main tools used for surface analyses, and studies have evolved two principal aims: on one hand, focusing on the origin and mechanisms of the Raman enhancement or on the magnitude of the SERS enhancement factor, and on the other hand, focusing on the direct use of the SERS intensity of the target molecule for analytical purposes. Regarding the first issue, the magnitude of the SERS enhancement is a very important aspect to be considered in order to understand the origin of the SERS signal and the nature of the SERS mechanisms. The main contribution to SERS enhancement is due to the huge electromagnetic field induced by the localized surface plasmon resonances (LSPRs) of their nanometric particles or clusters [4,5], and this singular characteristic makes possible its wide use for the study of many organic molecules adsorbed on colloidal metal solutions and substrates. Therefore, the high sensitivity of this technique allows detailed information to be obtained concerning the adsorbed species at very low concentrations that is directly related to their adsorption mechanism. Now, fifty years after the discovery of the SERS phenomenon, its applications have experienced a huge increase with an improvement in substrates and devices at the nanoscale level in different fields, for example, biochemistry and biosensing, catalysis, and electrochemistry [6–8]. However, the systematic interpretation of a particular SERS spectrum can be a challenge, given that different surface selection

rules have been proposed in order to explain the selective enhancement of the SERS bands. The most commonly used SERS rules are derived from the so-called electromagnetic enhancement mechanism (EM), which allows us to guess the orientation and geometrical configuration of an adsorbate on a metal surface [9,10]. Far more complex selection rules are derived from additional enhancement mechanisms related to resonance Raman effects involving excited electronic states of the molecule (surface-enhanced resonant Raman scattering, SERRS), metal–adsorbate photoinduced charge transfer (CT) processes, or other electronic resonances of the surface complex [11–13]. Depending on the particular molecule–metal system studied and on the experimental conditions, these mechanisms can operate simultaneously; in these circumstances, it is difficult to recognize each one and to evaluate their relative contribution to the enhancement of a certain spectrum.

In the present work, we focused the discussion on the experimental and theoretical SERS spectra of the organic compound p-aminothiophenol (PATP, HS-Ph-NH₂) recorded on silver and gold nanoparticles. This molecule has become a target molecule for checking the enhancement capability of different SERS substrates due to its very intense SERS spectra in a large number of investigations [14–17]. Additionally, due to the fact that the SERS spectrum of PATP on metal substrates is significantly different from its ordinary Raman spectrum, a historical discussion started almost a decade ago to try to explain its adsorption due to the formation of a new species, namely p,p′-dimercaptoazobenzene (DMAB) [18,19]. The presence of a new compound after adsorption is quite common in surface spectroscopies and, especially in some SERS studies, chemical transformations have taken place, e.g., polymerizations, isomerizations, or dehydrogenation [20–22]. However, the features of the SERS spectra of PATP are strongly dependent on many factors, such as the laser power density, the laser wavelength, the exposure time, the surface roughness, and the concentration of the molecule [18,19,23]. Although all of these factors determine the final SERS spectrum of PATP, there are still important aspects to understand, e.g., the effect of the morphology of the nanoparticles, together with the effect of the concentration of the PATP, which have not received great attention in published papers. In a previous work, we found that the SERS spectra of PATP on a silver electrode were dependent on the adsorbate concentration and dominated by a resonant charge transfer (CT) mechanism, where the charge was always transferred from the adsorbate to the metal [23]. Furthermore, we observed that the Raman signals of the SERS recorded at a low concentration arose from at least three different molecular species, but we analyzed the SERS signal only at 785 nm. In the present work, we delved further into the visible excitation range and recorded the SERS spectra of PATP on silver nanoparticles obtained by different procedures at 532 nm, which were also capable of detecting DMAB dimers and analyzing the adsorption behavior of this adsorbate in depth. In order to compare the SERS results with previous work in which we recorded the SERS spectra of PATP on a silver electrode, we also analyzed the effect of the concentration of PATP and the experimental SERS spectra were associated with the calculated Raman spectra of different silver complex species of PATP.

2. Materials and Methods

2.1. Chemicals and Instruments

All the reagents used in this work were purchased from Sigma-Aldrich with purity grades up to 99%. In the case of p-aminothiophenol, the purity grades were up to 97%. All the solutions were prepared by using Milli-Q-quality water (resistivity over 18 MΩcm).

UV–Vis spectra were acquired with an Agilent 8453 UV–Vis spectrophotometer. Raman and SERS spectra were recorded using a Renishaw Invia Qontor micro-Raman spectrometer equipped with a charge-coupled device (CCD) camera, employing the following different excitation lines: 488 nm, 532 nm, and 785 nm. The resolution was set to 2 cm^{−1} and the geometry of the micro-Raman measurements was 180°. In the case of liquid samples, a quartz cell with a 1 cm path length was used and the solid samples were directly analyzed through the microscope by using the Renishaw-specific macro device. This macro-cell system was equipped with an objective with a focal length of 30 mm (NA = 0.17), which

caused a laser spot of 3.82 μm at 532 nm and 5.63 μm at 785 nm. The output of the laser was set to 100% of its power in both cases, giving rise to approximately 5 mW at the 532 nm and 28 mW at the 785 nm excitation line on the sample place.

Transmission electron microscopy (TEM) images were obtained using a JEOL JEM 1400 (JEOL, Tokyo, Japan) microscope working at 80 kV.

2.2. Preparation of Silver Colloids

Two different silver colloids were prepared. Ag-BH was obtained according to the method described by J.A. Creighton et al. [24], which basically consists of reducing one volume of 10^{-3} M AgNO_3 with three volumes of 2×10^{-3} M NaBH_4 that has been previously cooled to a temperature between 0 and 5 $^\circ\text{C}$. The Ag-Hx colloid was prepared using the method of N. Leopold et al. [25], in which AgNO_3 was reduced by hydroxylamine hydrochloride in a slightly alkaline medium, so that the proportion of hydroxylamine hydrochloride/silver nitrate was chosen to obtain concentrations of $1.5 \times 10^{-3}/10^{-3}$ M in the final reaction mixture. Additionally, we followed one of the procedures proposed by these authors as follows: we added 10 mL of hydroxylamine/sodium hydroxide dropwise to 90 mL of silver nitrate. Figure 1 shows the absorbance spectra of the silver colloids of nanoparticles obtained by using methods presented above, together with their corresponding images.

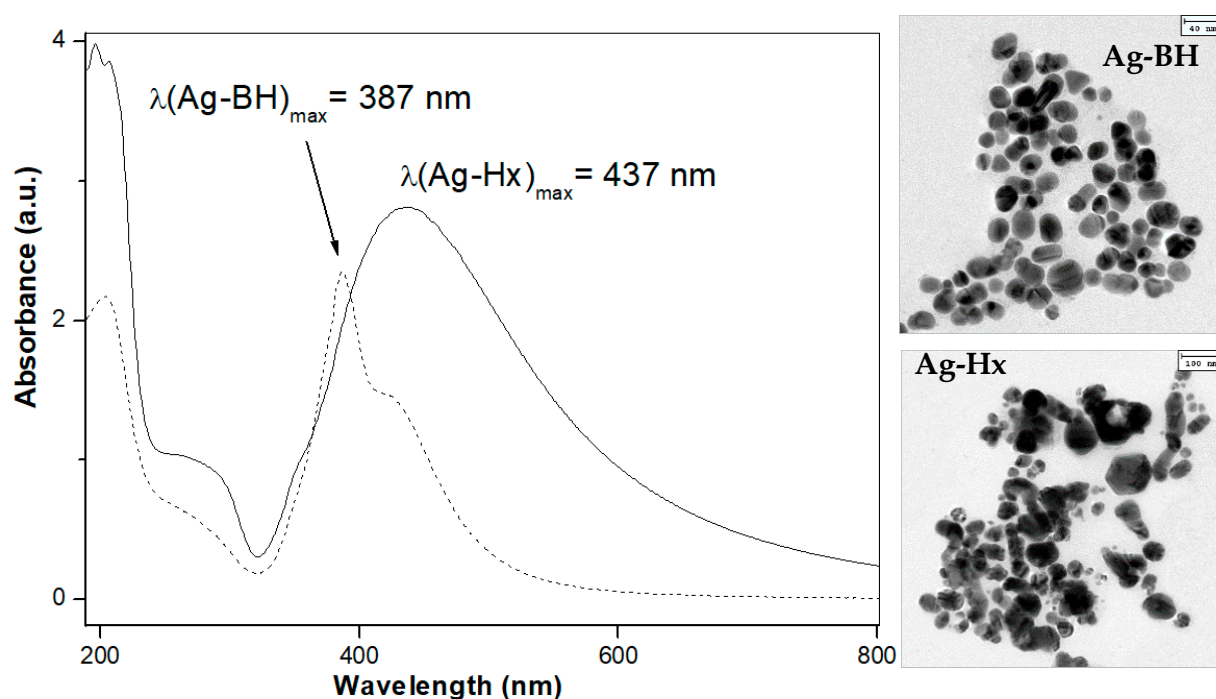


Figure 1. UV-Vis absorption spectra of Ag-BH and Ag-Hx silver colloids and their corresponding TEM images.

2.3. Theoretical Calculations

All the calculations carried out in this study were performed using the Gaussian 16 suite of programs [26]. The GaussView 5.0 software [27] was used for pre-processing, structure modification, and post-processing analyses of structures, frequencies, and forces. The B3LYP functional with the Pople-type basis set (6-311++G (d,p)) was applied. The PATP and DMAB molecular structures were optimized and no imaginary frequencies were found. In the case of silver complexes, the optimization was carried out with the use of the same DFT method coupled with a mixed basis set: 6-311++G (d,p) for C, O, and H atoms and LanL2DZ for silver. For the TD-DFT, a hybrid functional B3LYP was used with the same mixed basis sets.

3. Results

The UV–Vis spectra of both the silver colloids represented in Figure 1 exhibited a band in the visible region around 400 nm, with a maximum at 387 nm and 437 nm, near the resonance with the 532 nm excitation line, but far away from the NIR excitations. However, when PATP adsorbed onto these colloids, the corresponding absorption maximum was red-shifted and a secondary maximum arose around 800 nm, allowing overlap between the excitation wavelengths and the SERS spectra at both laser lines. Figure 2 shows the UV–Vis absorption spectra of PATP on Ag-BH and Ag-Hx at different concentrations, and we observed a secondary maximum around 768 nm on Ag-BH and around 861 nm on Ag-Hx when the concentration of PATP was 10^{-5} M or 10^{-6} M in both cases.

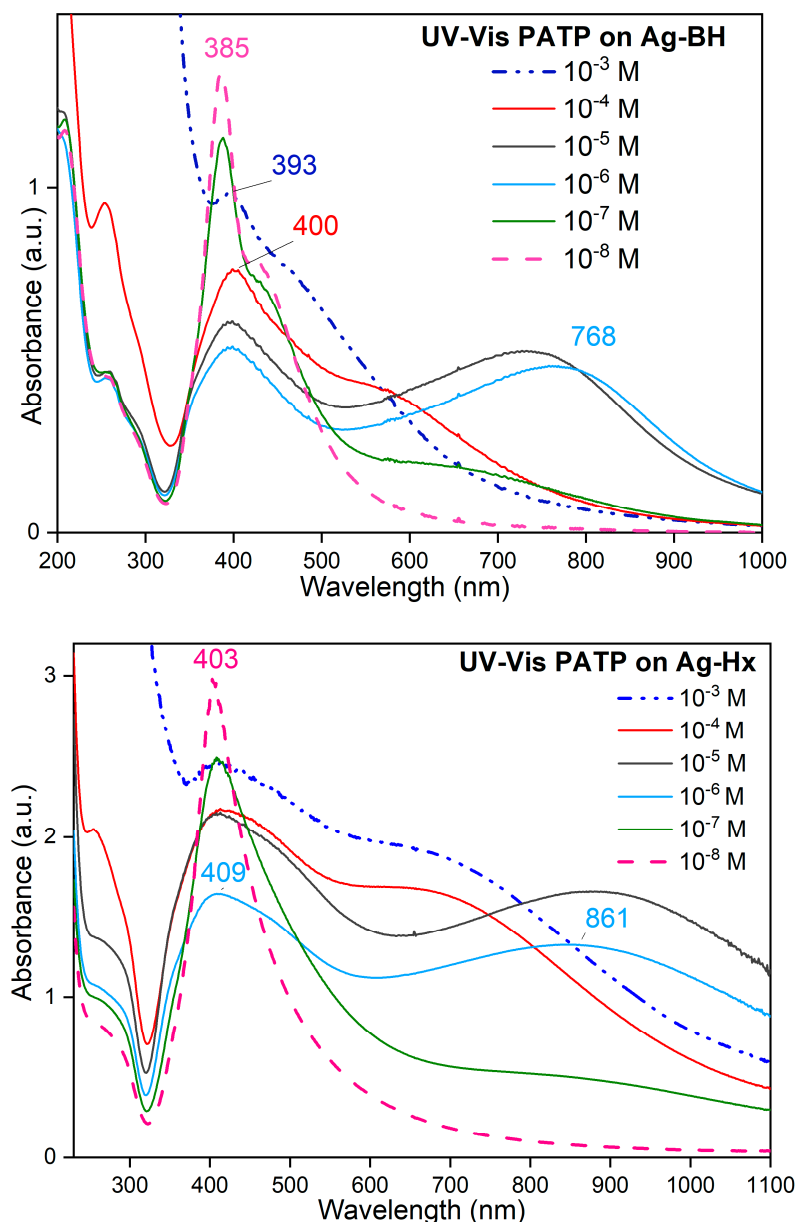


Figure 2. UV–Vis absorption spectra of PATP on Ag-BH and Ag-Hx at different concentrations.

Figure 3 shows the SERS spectra of PATP obtained at several concentrations on the Ag-BH and Ag-Hx silver colloids. Despite these colloids having different morphologies and sizes of nanoparticles, as can be observed in Figure 1, the SERS spectra of PATP underwent a similar behavior in both cases. At a cursory glance, it can be observed in Figure 3 that the SERS bands of PATP recorded at 532 nm were different from those obtained by exciting in

the NIR at 785 nm. This is a very characteristic behavior of this molecule because of the azo dimerization of PATP [19]. The specific bands from DMAB can be observed on both silver colloids at 532 nm, acquired at 1574, 1435, 1391, and 1144 cm^{-1} . The strong peaks around 1391 cm^{-1} and 1435 cm^{-1} (recorded at a low concentration) are related to the N=N vibration of DMAB, so their intensity can best describe the formation of DMAB [19,28].

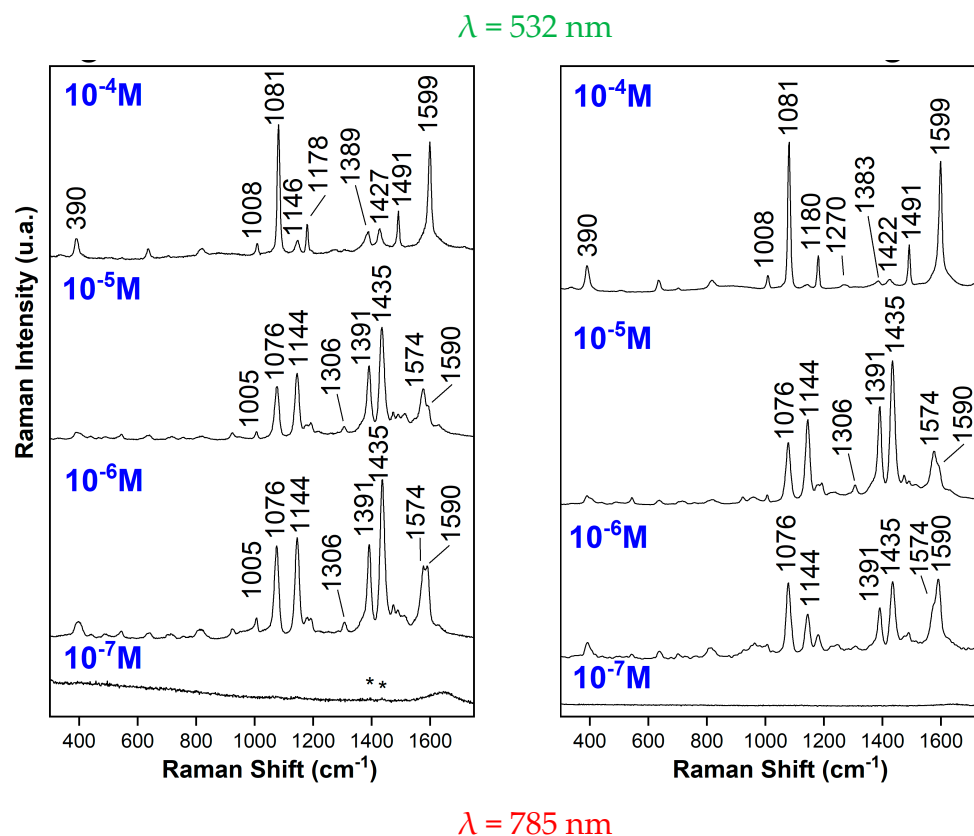
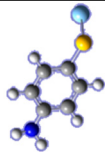
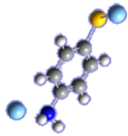
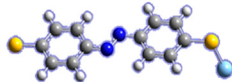
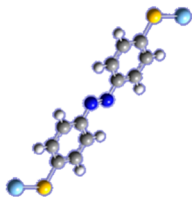


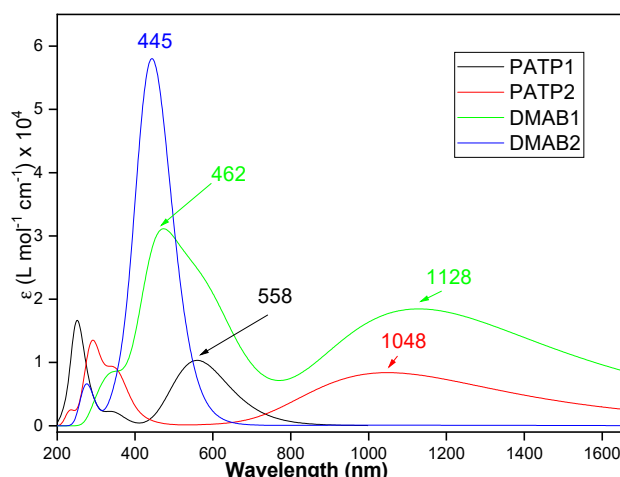
Figure 3. SERS spectra of different concentrations of PATP on Ag-BH (left) and Ag-Hx (right) at 532 nm and 785 nm excitation wavelengths. Note (*) as PATP bands.

The SERS band at 1076 cm^{-1} is due to the C-S stretching vibration, which can be generated by both PATP and DMAB with a comparable intensity. Interestingly, as we observed in Figure 3, the SERS bands of DMAB exhibited a higher enhancement when we recorded the SERS at a lower concentration. It is also very fascinating that the SERS of DMAB species was detected at 532 nm, but it was almost imperceptible at 785 nm, and was only detectable when we recorded the SERS spectra of PATP at a very low concentration, i.e., 10^{-6} M or 10^{-7} M. In this sense, the limit of detection (LOD) was lower when we recorded the SERS spectra at 785 nm, and in this case, the most intense SERS bands belonged to the PATP species. These results show that the dimerization process is favored at low concentrations, perhaps because of more active sites being available on the metal surface. The same behavior was observed on both the silver colloids.

In order to clarify the adsorbed chemical species of PATP that give rise to the SERS spectrum, DFT calculations for different silver complexes of PATP and DMAB were performed and their Raman spectra were compared with the experimental one. Therefore, Table 1 shows the corresponding species considered for this study and the UV-Vis plot for the first excited state from the TD-DFT calculations that were used to simulate the UV spectra and to determine the MOs involved in each transition [29].

Table 1. Optimized geometries of PATP and DMAB silver complexes and UV–Vis plot for the first excited state from the TD-DFT calculations of each silver complex.

	PATP1	PATP2
Optimized structures		
UV–Vis λ_{\max} , nm	558 H -> L (70%)	1048 H -> L (73%)
	DMAB1	DMAB2
Optimized structures		
UV–Vis λ_{\max} , nm	462 H -> L + 1 (58%)	445 H -> L + 2 (67%)



Symbols: λ_{\max} : wavelength of maximum absorbance; H: HOMO orbital; L: LUMO orbital.

A simulation of the experimental SERS spectra was performed at 532 nm and 785 nm by applying an average algorithm of several curves from the theoretical spectrum of each species (see Figure 4) using the OriginPro 2023b SR1 [30]. In Figure 4, a very good similarity can be observed between the experimental and the theoretical spectra by combining different percentages of the whole Raman intensity of each species. Based on these theoretical results, it was confirmed that the main species that contribute to the SERS signal at 532 nm are DMAB1 and DMAB2, and in the case of the SERS recorded at 785, it was mainly the PATP1 species.

As has been seen previously, the intensity of the SERS signal of monomer (PATP) or dimer (DMAB) species is sensitive to the excitation wavelength, and this fact was supported by the use of the DFT calculation, as shown in Figure 4.

These calculations were performed with the B3LYP functional methods. It was observed that the theoretical absorption electronic spectra of dimer species had lower wavelengths than those of the PATP. This fact means that PATP silver complexes will preferentially be SERS-active at higher wavelengths, which fits quite well with the experimental SERS results shown in Figure 3. It was established that, when recording the spectra at 532 nm, we obtained a more intricate SERS spectrum coming from the DMAB mixture of at

least two metal complexes, and when we recorded at 785 nm, we basically obtained the SERS of the PATP adsorbed mainly through the sulfur atom.

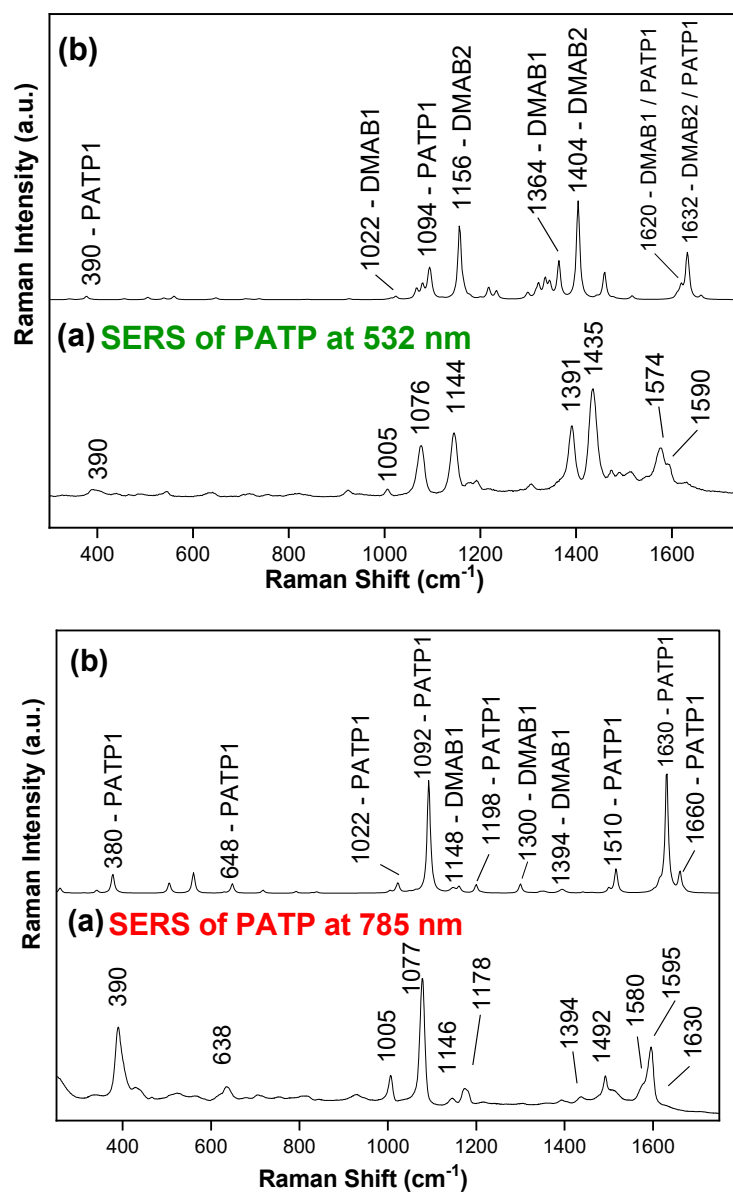


Figure 4. Theoretical average of different PATP and DMAB Raman spectra and experimental SERS spectra of PATP 10^{-5} M on Ag-BH recorded at 532 nm and 785 nm.

On the other hand, the presence of different species adsorbed onto the metal surface gave rise to the acquisition of simultaneous SERS signals from those species and the consequent overlapping of some bands. This was the case for the aromatic vibrational mode 8a, around 1600 cm^{-1} , which was a very characteristic SERS band that was acquired simultaneously from DMAB and PATP at 532 nm. In this wavenumber range, it was also observed that the SERS bands split when there was a greater contribution of DMAB (see Figure 4b at 532 nm). This was due to the asymmetry of the aromatic rings of the dimer when it was linked to the surface through one sulfur atom, generating the theoretical SERS bands at 1620 cm^{-1} and 1632 cm^{-1} , which were related to the experimental SERS bands at 1574 cm^{-1} and 1590 cm^{-1} , respectively. In SERS spectroscopy, it is very common that, when a molecule is adsorbed onto a metal surface, there is a break in the molecular symmetry, generating new bands that were not observed before.

4. Conclusions

The SERS spectra of PATP obtained at several concentrations and different wavelengths on Ag-BH and Ag-Hx silver colloids were analyzed. It was observed that the SERS spectra were quite similar for both metal colloids, with only some small differences regarding the relative intensities, and the SERS bands of DMAB exhibited a higher enhancement when we recorded the lower SERS at 532 nm. The dimer was almost imperceptible at 785 nm, and was only detectable when the SERS spectra of PATP were recorded at a very low concentration, i.e., 10^{-6} M or 10^{-7} M. Based on these results, it can be concluded that the dimerization process is favored at low concentrations due to the presence of more active sites available on the metal surface. Considering the theoretical simulation of the SERS spectra, it has been demonstrated that, when the spectra at 532 nm were acquired, we obtained a more intricate SERS spectrum coming from a DMAB mixture of at least two metal complexes. However, when the SERS spectra of PATP were acquired at 785 nm, we basically obtained the SERS of the PATP species adsorbed mainly through the sulfur atom.

Author Contributions: Conceptualization, methodology, and investigation: M.R.L.-R.; theoretical calculations: M.R.L.-R.; Raman spectroscopy measurements and investigation: L.G.-G.; writing, reviewing, and editing: all authors. All authors have read and agreed to the published version of the manuscript.

Funding: R.C.-C. acknowledges funding from the “Ramón y Cajal” fellowship from the Ministerio de Ciencia e Innovación, grant number RyC 2021-03447-I.

Institutional Review Board Statement: Not applicable.

Informed Consent Statement: Not applicable.

Data Availability Statement: The data presented in this study are available from the corresponding author upon request.

Acknowledgments: The authors thank the laboratory of AFM and Raman microscopy at the SCAI (Central Services Research Support) of the University of Málaga (Spain) and Rafael Larrosa (University of Málaga) for the use of their computational facilities.

Conflicts of Interest: The authors declare no conflicts of interest.

References

1. Fleischmann, M.; Hendra, P.J.; McQuillan, A.J. Raman spectra of pyridine adsorbed at a silver electrode. *Chem. Phys. Lett.* **1974**, *26*, 163–176. [[CrossRef](#)]
2. Jeanmaire, D.L.; Van Duyne, R.P. Surface Raman spectroelectrochemistry. *J. Electroanal. Chem.* **1977**, *84*, 1–20. [[CrossRef](#)]
3. Albrecht, M.G.; Creighton, J.A. Anomalous intense Raman spectra of pyridine at a silver electrode. *J. Am. Chem. Soc.* **1977**, *99*, 5215–5217. [[CrossRef](#)]
4. Aroca, R. *Surface-Enhanced Vibrational Spectroscopy*; John Wiley & Sons, Ltd.: West Sussex, UK, 2006.
5. Moskovits, M. Persistent Misconceptions Regarding SERS. *Phys. Chem. Chem. Phys.* **2013**, *15*, 5301–5311. [[CrossRef](#)] [[PubMed](#)]
6. Kerker, M. *Selected Papers on Surface-Enhanced Raman Scattering*; SPIE Milestone Series; Thompson, B.J., Ed.; SPIE: Bellingham, WA, USA, 1990.
7. Kneipp, K.; Kneipp, H.; Itzkan, I.; Dasari, R.R.; Feld, M.S. Ultrasensitive Chemical Analysis by Raman Spectroscopy. *Chem. Rev.* **1999**, *99*, 2957–2976. [[CrossRef](#)] [[PubMed](#)]
8. Pettinger, B.; Picardi, G.; Ertl, G. Surface Enhanced Raman Spectroscopy: Towards Single Molecule Spectroscopy. *Electrochemistry* **2000**, *68*, 942–949. [[CrossRef](#)]
9. Moskovits, M.; DiLella, D.P.; Mainard, K.J. Surface Raman spectroscopy of a number of cyclic aromatic molecules adsorbed on silver: Selection rules and molecular. *Langmuir* **1988**, *4*, 67–76. [[CrossRef](#)]
10. Creighton, J.A. The Selection Rules for Surface-Enhanced Raman Spectroscopy. In *Spectroscopy of Surfaces*; Clark, R.J.H., Hester, R.E., Eds.; Wiley: Chichester, UK, 1988; pp. 37–89.
11. Otto, A.; Mrozek, I.; Grabhorn, H.; Akemann, W. Surface-enhanced Raman. *J. Phys. Condens. Matter* **1992**, *4*, 1143–1212. [[CrossRef](#)]
12. Arenas, J.F.; Lopez-Tocon, I.; Otero, J.C.; Marcos, J.I. Charge Transfer Processes in Surface-Enhanced Raman Scattering. Franck–Condon Active Vibrations of Pyridine. *J. Phys. Chem.* **1996**, *100*, 9254–9261. [[CrossRef](#)]
13. Arenas, J.F.; Woolley, M.S.; Otero, J.C.; Marcos, J.I. Charge-Transfer Processes in Surface-Enhanced Raman Scattering. Franck–Condon Active Vibrations of Pyrazine. *J. Phys. Chem.* **1996**, *100*, 3199–3206. [[CrossRef](#)]

14. Wang, Y.; Zou, X.; Ren, W.; Wang, W.; Wang, E. Effect of Silver Nanoplates on Raman Spectra of p-Aminothiophenol Assembled on Smooth Macroscopic Gold and Silver Surface. *J. Phys. Chem. C* **2007**, *111*, 3259–3265. [[CrossRef](#)]
15. Sun, M.; Huang, Y.; Xia, L.; Chen, X.; Xu, H. The pH Controlled Plasmon-Assisted Surface Photocatalysis Reaction of 4-Aminothiophenol to p,p'-Dimercaptoazobenzene on Au, Ag, and Cu Colloids. *J. Phys. Chem. C* **2011**, *115*, 9629–9636. [[CrossRef](#)]
16. Gabudean, A.M.; Biro, D.; Astilean, S. Localized Surface Plasmon Resonance (LSPR) and Surface-Enhanced Raman Scattering (SERS) Studies of 4-Aminothiophenol Adsorption on Gold Nanorods. *J. Mol. Struct.* **2011**, *993*, 420–424. [[CrossRef](#)]
17. Zong, S.; Wang, Z.; Yang, J.; Cui, Y. Intracellular pH Sensing Using p-Aminothiophenol Functionalized Gold Nanorods with Low Cytotoxicity. *Anal. Chem.* **2011**, *83*, 4178–4183. [[CrossRef](#)] [[PubMed](#)]
18. Osawa, M.; Matsuda, N.; Yoshii, K.; Uchida, I. Charge-Transfer Resonance Raman Process in Surface-Enhanced Raman-Scattering from p-Aminothiophenol Adsorbed on Silver Herzberg-Teller Contribution. *J. Phys. Chem.* **1994**, *98*, 12702–12707. [[CrossRef](#)]
19. Huang, Y.-F.; Zhu, H.-P.; Liu, G.-K.; Wu, D.-Y.; Ren, B.; Tian, Z.-Q. When the Signal Is Not from the Original Molecule to Be Detected: Chemical Transformation of para-Aminothiophenol on Ag during the SERS Measurement. *J. Am. Chem. Soc.* **2010**, *132*, 9244–9246. [[CrossRef](#)]
20. Suh, J.S.; Michaelian, K.H. Surface-enhanced Raman scattering as a probe of surface geometry effects on the polymerization of an acrylic acid on silver. *J. Phys. Chem.* **1987**, *91*, 598–600. [[CrossRef](#)]
21. Chun, H.A.; Yi, S.S.; Kim, M.S.; Kim, K. Adsorption and reaction of 4-methoxycinnamionitrile on a silver surface: A surface-enhanced Raman spectroscopic study. *J. Raman Spectrosc.* **1990**, *21*, 743–749. [[CrossRef](#)]
22. Castro, J.L.; Lopez Ramirez, M.R.; Lopez Tocon, I.; Otero, J.C. Surface-enhanced Raman scattering of 3-phenylpropionic acid (hydrocinnamic acid). *J. Raman Spectrosc.* **2002**, *33*, 455–459. [[CrossRef](#)]
23. Lopez-Ramirez, M.R.; Aranda-Ruiz, D.; Avila-Ferrer, F.J.; Centeno, S.P.; Arenas, J.F.; Otero, J.C.; Soto, J. Analysis of the Potential Dependent Surface-Enhanced Raman Scattering of p-Aminothiophenol on the Basis of MS-CASPT2 Calculations. *J. Phys. Chem. C* **2016**, *120*, 19322–19328. [[CrossRef](#)]
24. Creighton, J.A.; Blatchford, C.G.; Albrecht, M.G. Plasma resonance enhancement of Raman scattering by pyridine adsorbed on silver or gold sol particles of size comparable to the excitation wavelength. *J. Chem. Soc. Faraday Trans. II* **1979**, *75*, 790–798. [[CrossRef](#)]
25. Leopold, N.; Lendl, B. A New Method for Fast Preparation of Highly Surface-Enhanced Raman Scattering (SERS) Active Silver Colloids at Room Temperature by Reduction of Silver Nitrate with Hydroxylamine Hydrochloride. *J. Phys. Chem. B* **2003**, *107*, 5723–5727. [[CrossRef](#)]
26. Frisch, M.J.; Trucks, G.W.; Schlegel, H.B.; Scuseria, G.E.; Robb, M.A.; Cheeseman, J.R.; Scalmani, G.; Barone, V.; Petersson, G.A.; Nakatsuji, H.; et al. *Gaussian 16. Revision C.01*; Gaussian Inc.: Wallingford, CT, USA, 2016.
27. Dennington, R.; Keith, T.A.; Millam, J.M. *GaussView, Version 6*; Semichem Inc.: Shawnee Mission, KS, USA, 2016.
28. Huang, Y.Z.; Fang, Y.R.; Yang, Z.L.; Sun, M.T. Can p,p'-Dimercaptoazobisbenzene Be Produced from p-Aminothiophenol by Surface Photochemistry Reaction in the Junctions of a Ag Nanoparticle–Molecule–Ag (or Au) Film? *J. Phys. Chem. C* **2010**, *114*, 18263–18269. [[CrossRef](#)]
29. Cojocaru, C.; Airinei, A. Molecular structure and modeling studies of azobenzene derivatives containing maleimide groups. *SpringerPlus* **2013**, *2*, 586. [[CrossRef](#)] [[PubMed](#)]
30. OriginPro. *Version 2023b*; OriginLab Corporation: Northampton, MA, USA, 2023.

Disclaimer/Publisher's Note: The statements, opinions and data contained in all publications are solely those of the individual author(s) and contributor(s) and not of MDPI and/or the editor(s). MDPI and/or the editor(s) disclaim responsibility for any injury to people or property resulting from any ideas, methods, instructions or products referred to in the content.